Determining fractal parameter and depth of magnetic sources for Ardabil geothermal area using aeromagnetic data by de-fractal approach

A. Khojamli[1*], F. Doulati Ardejani[2], A. Moradzadeh[2], A. Nejati Kalate[1], A. Roshandel Kahoo[1] and S. Porkhial[3]

1. School of Mining, Petroleum & Geophysics Engineering, Shahrood University of Technology, Shahrood, Iran
2. School of Mining Engineering, College of Engineering, University of Tehran, Tehran, Iran
3. Department of geothermal energy, Renewable Energy Organization of Iran, Ministry of Energy, Tehran, Iran

Abstract
The Ardabil geothermal area is located in the northwest of Iran, which hosts several hot springs. It is situated mostly around the Sabalan Mountain. The Sabalan geothermal area is now under investigation for the geothermal electric power generation. It is characterized by its high thermal gradient and high heat flow. In this study, our aim is to determine the fractal parameter and top and bottom depths of the magnetic sources. A modified spectral analysis technique named "de-fractal spectral depth method" is developed and used to estimate the top and bottom depths of the magnetized layer. A mathematical relationship is used between the observed power spectrum (due to fractal magnetization) and an equivalent random magnetization power spectrum. The de-fractal approach removes the effect of fractal magnetization from the observed power spectrum, and estimates the parameters of the depth to top and depth to bottom of the magnetized layer using the iterative forward modelling of the power spectrum. This approach is applied to the aeromagnetic data of the Ardebil province. The results obtained indicated variable magnetic bottom depths ranging from 10.4 km in the northwest of Sabalan to about 21.1 km in the north of the studied area. In addition, the fractal parameter was found to vary from 3.7 to 4.5 within the studied area.

Keywords: *Fractal Parameter, Aeromagnetic Data, Geothermal Field, Magnetic Field Sources, Power Spectrum, Sabalan.*

1. Introduction
The interpretation of potential fields is generally carried out in the frequency domain due to (1) simplicity in the implementation of signal processing tools, and (2) easy and concise characterization of potential field signals caused by a large variety of source models. In the frequency domain, the geophysical source parameters such as density have been assumed as uncorrelated distribution. To the contrary, source distribution of the physical parameters is correlated following the scaling or fractal laws. Mandelbrot (1983) has introduced the concept of fractal noises, which provides a realistic model for the power spectral density of various parameters in nature [1]. Fractal source distributions have power spectra proportional to $k^{-\beta}$, where k is the wave number (i.e. length of the wave vector) and β denotes the respective fractal parameter. This has been discovered by the detailed analysis of the densities and susceptibilities of several borehole data around the world including the German continental deep drilling program in southeastern Germany. The fractal parameter reflects the proportion of long and short wavelength variations of a signal. The higher the value of the fractal parameter, the stronger is the relative intensity of the long wavelength variations of the signal.

The fractal parameter values depend upon the lithology and heterogeneity of the subsurface [2]. Fedi et al. (1997) have suggested correcting the power spectrum by $k^{-2.9}$ before calculating the

depth values because the method introduced by Spector and Grant (1970) has an inherent power-law relation [3, 4]. The inversion approach based on the fractal distribution of the sources suggests simultaneously estimating the proportionality constant, fractal parameter, and depth from the power spectrum [5-8].

However, a simultaneous estimation of the depth and fractal parameters is difficult because of the interrelation of these parameters [9, 10]. Bouligand et al. (2009) have suggested fixing the fractal parameter to calculate the depth from the magnetic field sources due to the interrelation of the fractal and depth parameters [10]. First, they constrained the depth to the bottom of magnetic sources by heat-flow data. Then they calculated the fractal parameter. They used a constant value of 3 on the fractal parameter for computing the Curie depth for the western United States from the method proposed by Maus et al. (1997) [8]. Bouligand et al. (2009) have also reviewed the fractal parameter derived from the aeromagnetic studies in continental domains, and found a large range of values (Table 1) [10].

Table 1. Summary of published estimates for fractal parameter within various contexts and from spectral analysis of aeromagnetic maps.

β	Lithology	Location	Reference
1.5	Sedimentary	Bohemian Massif, Germany	Maus and Dimri (1995)
2.8	Metamorphic	Bohemian Massif, Germany	Maus and Dimri (1995)
3.0	Igneous	Bohemian Massif, Germany	Maus and Dimri (1995)
3.2	Metamorphic covered by sediments	Sakatchewan, Canadian shield	Maus and Dimri (1996)
3.8	Metamorphic and Intrusive	Ontario, Canadian shield	Gregotski et al. (1991)
3.9	Metamorphic covered by sediments	Sakatchewan, Canadian shield	Gregotski et al. (1991)
4.0	Metamorphic covered by sediments	Sakatchewan, Canadian shield	Pilkington et al. (1994)
4.0	Variable	Canadian shield	Pilkington and Todoeschuck (1993)
4.1	Metamorphic	Ontario, Canadian shield	Gregotski et al. (1991)
4.0	Variable	Central Asia	Maus et al. (1997)
4.0	Principally Igneous	South Africa (with LIP Karoo)	Maus et al. (1997)
5.5-5.8	Igneous	Hawaii	Maus and Dimri (1996)

The main objective of the current work was to develop an algorithm for estimation of the fractal parameter using a de-fractal spectral analysis of the magnetic data in order to determine the bottom depth of magnetic sources. This approach of analysis of magnetic data assumes that the observed power spectrum is equivalent to the random magnetization model multiplied by the effect of fractal magnetization. It is believed that the de-fractal method can reduce the ambiguity related to the selection of the fractal parameter to provide the bottom depth estimates that are more reasonable than those estimated using conventional methods. However, the ability of the de-fractal method has not been verified so much for practical exploration data. Hence, in this work, an attempt was made to use this approach to remove the effect of fractal magnetization from the power spectrum of real magnetic data to have a reasonable depth estimate of magnetic sources.

2. Spectral analysis

In the last four decades, various methods have been developed and applied to estimate the depth to the bottom of magnetic sources using the averaged Fourier spectra of magnetic anomalies (e.g. [3, 4, 8-12]). The mathematical formulae of these methods are based on the assumptions of flat layers with particular distributions of magnetization including 1) random magnetization, and 2) fractal magnetization.

2.1. Random magnetization

Two methods are commonly used in the spectral estimation of the depth to the bottom of a magnetic anomaly based on random magnetization [9]: (a) the spectral peak method, which was originally given in an innovatory paper by Spector and Grant (1970), and used by Shuey et al. (1977), Blakely (1988) and Salem et al. (2000) among others, and (b) the centroid method, which was originally presented by Bhattacharyya and Leu (1977) and used with certain caveats and variations by Okubo et al. (1985) and Tanaka et al. (1999) [4, 12-17].

The power spectrum *P* for a 2D assemblage of bodies can be expressed as [4, 18]:

$$P(k_x, k_y) = 4\pi^2 C_m^2 \varphi_m(k_x, k_y) |\Theta_m|^2 |\Theta_f|^2$$
$$e^{-2|k|Z_t} \times (1 - e^{-|k|(Z_b - Z_t)})^2 \tag{1}$$

where k_x and k_y are the wave numbers in the *x* and *y* directions; C_m represents a constant of proportionality; ϕ_m denotes the power spectrum of the magnetization; Θ_m and Θ_f are the directional factors related to the magnetization and geomagnetic fields, respectively; and Z_t and Z_b are referred to the top and bottom depths of the magnetic sources, respectively.

After annular averaging, Eq. 1 can be written as:

$$P(k) = A_1 e^{-2|k|Z_t} (1 - e^{-(Z_b - Z_t)})^2 \tag{2}$$

where A_1 is a constant [19]. Eq. 2 can be further simplified to compute the centroid depth Z_c of the magnetic source ([11, 12, 16]) from the low-wave number part of the power spectrum, as:

$$\ln(\frac{\sqrt{P(k)}}{k}) = A_2 - |k|Z_c \tag{3}$$

where A_2 represents a constant. Eq. 2 can also be simplified to compute the top of the magnetic sources Z_t by assuming that the signals from the source tops dominate the power spectrum [4, 11, 12]:

$$\ln(P(k)) = A_3 - 2|k|Z_t \tag{4}$$

where A_3 is a constant. Once the centroid depth is obtained from Eq. 3 and the estimate of the depth to the top of the source is obtained from Eq. 4, the depth to the bottom of the magnetic body can be simply calculated as follows:

$$Z_b = 2Z_c - Z_t \tag{5}$$

The above two methods assume a layer of random magnetization. In some cases, these methods may lead to incorrect determinations of the Curie isotherm depth/magnetic bottom if the layer shows the fractal magnetization behavior [20].

2.1.1. Forward modelling of spectral peak method

Many experts [e.g. Ravat, 2004; Finn and Ravat, 2004; Ross et al. 2004, and Ravat et al. 2007] have proposed forward modelling of the spectral peak to better estimate the bottom depth using Eq. 6 [9, 21-23]:

$$P(k) = C(e^{-|k|Z_t} - e^{-|k|Z_b})^2 \tag{6}$$

where constant C (the non-depth-dependent term) can be adjusted to shift the modelled curve up or down to fit the observed peak. The location of the spectral peak and the slope in the high wave number range are controlled by Z_b and Z_t, respectively. The combination of both Z_t and Z_b control the slope immediately adjacent to the peak [9]. The advantage of the forward modelling is that it allows one to fit the position and the width of the peak iteratively, match the adjacent part of the slope more precisely, and explore the model space. Based on the fit of the modelled spectra with the observed data, one may accept or reject the results obtained more confidently in this overall subjective process of fitting specific parts of the spectra.

Spector and Grant (1970), Connard et al. (1983), Blakely (1988), Tanaka et al. (1999), and Ross et al. (2006) have assumed that crustal magnetization is a completely random function of position characterized by a flat power density spectrum ($\beta = 0$) [4, 14, 17, 24, 25]. The magnetic power spectra should be corrected for fractal behavior before applying the Spector and Grant method for depth determination. Fedi et al. (1997) have compared the depth estimation with and without the correction factor $k^{-2.9}$ for a number of ensemble average depths, and have concluded that the method presented by Spector and Grant, without fractal behavior correction, consistently overestimates the depths over the range of 0-15 km [3].

2.2. Fractal magnetization

The idea of using the models with fractal magnetization distribution originates from the concept of self-similarity, which is consistent with the susceptibility logs, susceptibility surveys, and magnetic maps [1, 5, 7, 26, 27].

The theoretical power spectrum due to a slab of fractal magnetization distribution has been given by Maus et al. (1997) as follows [8]:

$$\ln[P(k_x, k_y)]d\theta = C - 2k_H z_t - k_H \Delta z - \beta \ln(k_H) +$$
$$\int_0^{2\pi} \ln[\int_0^{\infty} (\cosh(k_H \Delta z) - \cos(k_z \Delta z))(1 + \left(\frac{k_z}{k_H}\right)^2)^{-1-\frac{\beta}{2}} dk_z \tag{7}$$

where *C* is a constant. The orientation of the geomagnetic field appears only in the constant C [8]. $\vec{k}_H = (k_x, k_y)$ is the wave number in the

horizontal plane, $k_H = \left|\vec{k}_H\right|$ represents its norm, θ is its angle with respect to k_x, and β denotes the fractal parameter describing the degree of magnetization fractal. For example, $\beta = 1$ is very close to the random magnetization model assumed by Spector and Grant (1970), as quoted in Bouligand et al. (2009) [4, 10]. Higher β values represent increasingly correlated magnetization variations. An increase in the fractal parameter of magnetization increases the slopes of the power spectrum, and, generally, Z_t and Z_b would be overestimated if a lower fractal parameter was assumed.

3. De-fractal spectral depth determination method

The de-fractal method was initially proposed by Salem et al. (2014) [20]. It is based upon the assumption that the observed power spectrum is adequately represented by a simplification of the fractal magnetization power spectrum, where the magnetization in the *x* and *y* directions is fractal and is constant in the z direction. In this case, the observed power spectrum is equivalent to the result of power spectral density of the random magnetization model multiplied by $k^{-\alpha}$ such that:

$$P_F(k_x, k_y) = P_R(k_x, k_y) * k^{-\alpha} \qquad (8)$$

where $P_F(k_x, k_y)$ is the observed power spectrum, and $P_R(k_x, k_y)$ represents the power spectrum due to the random magnetization model, *k* is referred to the radial wave number, and α denotes the fractal parameter $\alpha = \beta - 1$, where β is the fractal parameter of magnetization [27]. If the value for α can be determined, one can perform a "de-fractal" process on the observed power spectrum by multiplying it by the factor k^{α} and extracting a power spectrum equivalent to the random magnetization version, as follows:

$$P_R(k_x, k_y) = P_F(k_x, k_y) * k^{\alpha} \qquad (9)$$

Having removed the fractal effect, one can treat the resulting de-fractal power spectrum as though it was the power spectrum of a random magnetization model. The present approach can be considered as a correction to the power spectrum of the magnetic field for the fractal distribution of magnetization [20].

The de-fractal method utilizes all the previous techniques, and integrates the spectral peak and centroid methods in an interactive forward modelling approach. We de-fractal the power spectrum by a range of *α* parameters, and examine them for under- or over-correction. The viable values for *α* are those where the expected peak is present in the de-fractal power spectrum. The correct *α* is selected based on the visual inspection of the fit between the de-fractal power spectrum and the modelled power spectrum.

Figure 1 shows a flowchart of the de-fractal approach for estimating Z_b. A tentative low value of *α* was first chosen, and then the de-fractal transformation was performed on the observed power spectrum. We then applied the fractal centroid method, estimated Z_t based on fitting the linear segment in the mid to high wave number range of the power spectrum, and estimated the centroid depth by fitting the linear segment in the low wave number range of the scaled power spectrum.
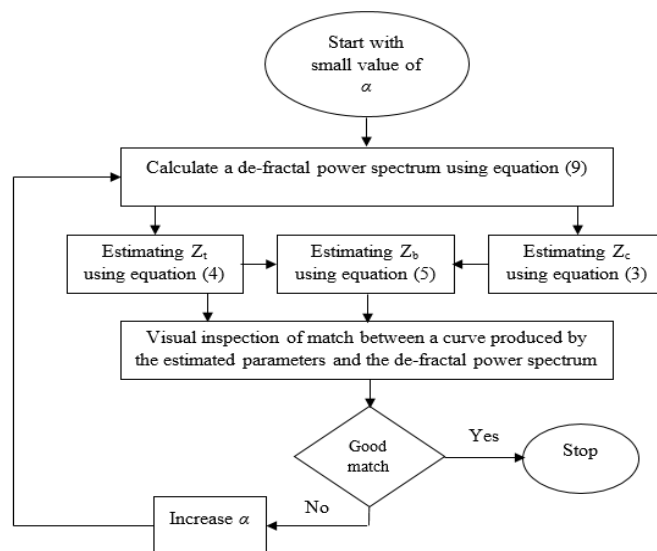
Figure 1. Flowchart of de-fractal approach for estimating depth to magnetic bottom (modified from [20]).

4. Fractal magnetization and depth to magnetic bottom in Ardabil province, northwest of Iran

Several hot springs with temperatures varying between 20 and 85 °C exist in the Ardabil region, which is mostly situated around the Sabalan Mountain (Mt. Sabalan). The geology of the Ardebil province is diverse and complicated, and has a long evolution history. These features discriminate the area from the other parts of Iran. North of Ardabil is covered with older alluvial, clay, marl, and tuff intercalations. The surrounding region around the Mt. Sabalan is characterized by the predominance of Quaternary terrace deposits (Dizu Formation), altered post-caldera Pleistocene Trachy-Andesitic domes, flows and lahars (Kasra Formation), unaltered syn-caldera Pleistocene Trachy-Dacite to Trachy-Andesitic flows, domes and lahars (Toas formation), and pre-caldera Trachy-Andesitic lavas, Tuffs, and pyroclastics (Valhazir formation) (Figure 2). The geological study of the northwest of Sabalan confirm that there are two major types of structural settings: a set of linear faults and several inferred-faults, and the faults strike predominantly toward the northwest and northeast [28, 29]. A northeast-southwest structural trend is dominant in the south of Ardebil city. The main geological units exposed in this area include Miocene's altered tuff, tuff breccia, pumice, travertine, sandstone, shale, marl, and conglomerate, and Eocene's olivine basalt and Trachy-Basalt which overlay volcanic breccia and trachy-andesite of Eocene age.

In this study, the aeromagnetic data acquired from the Geological Survey of Iran was used. This data was corrected for the International Geomagnetic Reference Field (IGRF 1976). To achieve the aim, the studied area was then divided into many square subregions. Selecting the optimal dimensions of these subregions is very important. The limited depth extent of the crustal magnetization would be visible in magnetic maps, covering less than $100*100 \text{ km}^2$ [8]. Okubo et al. (1985, 2003) have suggested the optimal dimensions of the investigated square window to be about 10 times the actual target depth [12, 30, 31]. Connard et al. (1983) have divided a magnetic data of the Cascade Range, central Oregon into overlapping blocks ($77 * 77 \text{ km}^2$), and calculated the radially average power spectrum for each block [24]. Tanaka et al. (1999) have divided the east and southeast Asia into subregions data (approximately $200 * 200 \text{ km}^2$), and estimated the power density spectra for each region [17]. Blakely (1988) has divided the

Nevada area into blocks ($120 * 120 \text{ km}^2$) in terms of magnetic or aeromagnetic data, and mapped the Curie point depth of Nevada State [14].

To select an appropriate block size for calculating the radial power spectra, a small program was written to calculate the radial power spectra for different window sizes, from 50 km to 400 km with 10 km increasing step size. The appropriate block size of $100 * 100 \text{ km}^2$ was then chosen so that the spectral peaks of the aeromagnetic data could be visible in the power spectrum. The absence of a peak indicates that the peak lies at wave numbers lower than the minimum resolved wave number, and that a larger window size is needed to compute the radial power spectrum and for detection to the bottom of the magnetic sources. Following that, 18 overlapping blocks of sizes $100 * 100 \text{ km}^2$ (overlapped fifty percent with the adjacent blocks) were extracted from the reduced to pole (RTP) aeromagnetic data of Ardabil area for estimating the depth to the top and bottom of the magnetic field sources using the de-fractal method (Figure 3).

For each block, the effects of very deep regional structures were removed using a first order trend filter, and grids were expanded by 10% using the maximum entropy method to make the edges continuous. Then power spectrum was calculated using the fast Fourier transform (FFT). Following that, the de-fractal method was applied to the power spectrum of each block using different α values, and associated values of Z_t and Z_b of the magnetic layer within the blocks were estimated based on the scheme shown in Figure 1. The selection of the most suitable wavelength band is very important and crucial for calculating the centroid and the top of the deepest anomalous sources. It always depends, to some extent, on personal judgment when fitting the straight line in the plot of logarithm of power spectrum *vs.* wave number. We found two types of blocks. For the first type, it was easy to determine the appropriate wavelength band because the plot of spectra depicted a linear segment that could be fitted to a straight line. For the second type, the selection of the wavelength band was more difficult. However, the wavelength band for computing the centroid and top depths from plots of the logarithm power spectrum *vs.* wave number was selected by looking for a nearly straight line in the plots.

Figure 4 shows an example of the de-fractal method for block 4. In this approach, to find an appropriate fractal value for depth calculation within each block, a set of fractal parameter values (α) starting from 1 to 6 with increment 0.1

were used. The top and bottom depths (Z_t and Z_b) were then estimated using Eqs. (4), (5), and (6) for each de-fractal power spectrum. Finally, the fitness of the modelled power spectrum with the nominated de-fractal spectrum was checked. According to good fit, the optimum fractal value was selected. Figure 4 displays how the match between the modelled power spectrum and the de-fractal spectrum improves gradually until a good fit is obtained using the fractal value $\alpha = 4.5$. The goodness of fit is assessed visually taking into account the main features along the whole power spectrum with particular focus on the longest wavelengths and ignoring local excursions in the power spectrum. To ensure that other possible solutions corresponding to higher values of fractal exponent are not missed, we used a higher fractal value of $\alpha = 5$, and determined Z_t and Z_b from the de-fractal centroid method as before. A mismatch was found between the modelled power spectrum and the de-fractal spectrum (Figure 4f). This indicates that the cross-checking between both the peak modelling and the centroid methods guards against the erroneous results.

Table 2 gives the estimated results for the fractal parameter α, depth to the top, and depth to the bottom of the magnetic source. For all blocks, the determined α values were between ($\alpha = 3.7$) and ($\alpha = 4.5$), whereas it had been shown earlier that this parameter varies within a large range in the continental domain [10]. We found different α values in the Ardabil area. This result is not surprising because the magnetic pattern of the

rocks in each block may be completely different from that in other blocks. The range of the magnetic bottom depths are from 10.4 km in the northwest of Sabalan to about 21.1 km in the north of the studied area (Figure 5).

5. Conclusions

In this work, we determined the depths to the magnetic bottom using the de-fractal spectral analysis method. This method applies a transformation to the observed magnetic field based on an estimated fractal parameter such that the power spectrum resembles the power spectrum that would be generated by a random magnetization distribution. The advantages of this method are that the range of the feasible de-fractal parameters can be estimated, and the depth to the bottom of the magnetic field sources or anomalies (magnetic sources) is obtained based on simultaneously estimating the depth values from the centroid method and visual inspection of the forward modelling of the spectral peak. The method was applied to 50% overlapping 18 blocks with 100 km * 100 km^2 dimensions of aeromagnetic data in Ardabil area. As a result, the fractal parameter was determined between 3.7 and 4.5. The results obtained also indicate that the depth to bottom of sources of the magnetic anomalies varies from 10.4 km in the northwest of Sabalan to about 21.1 km in the north of the studied area.
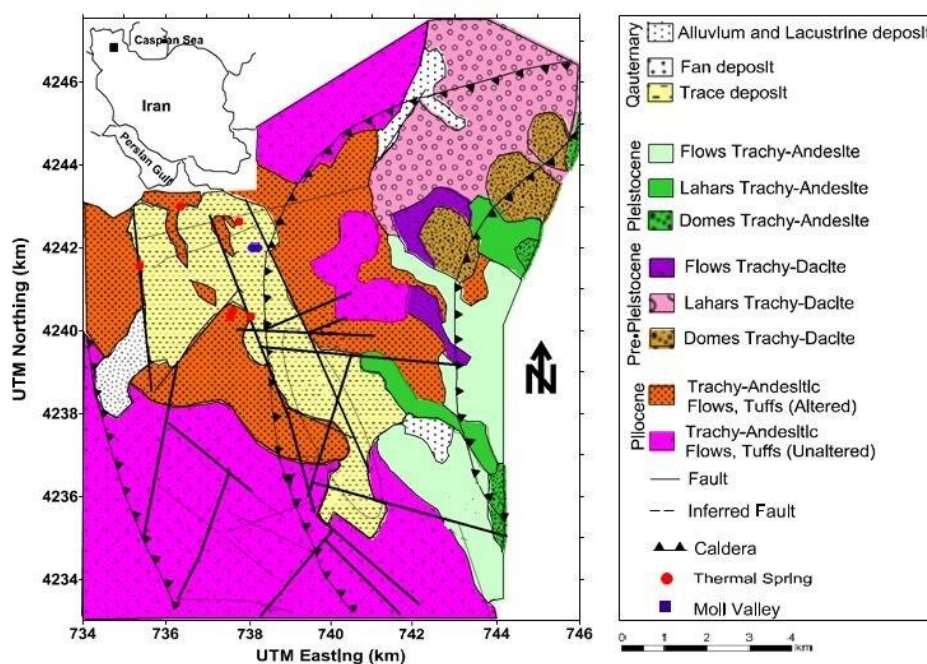
Figure 2. Geologic map of Sabalan geothermal field (modified from [32]).
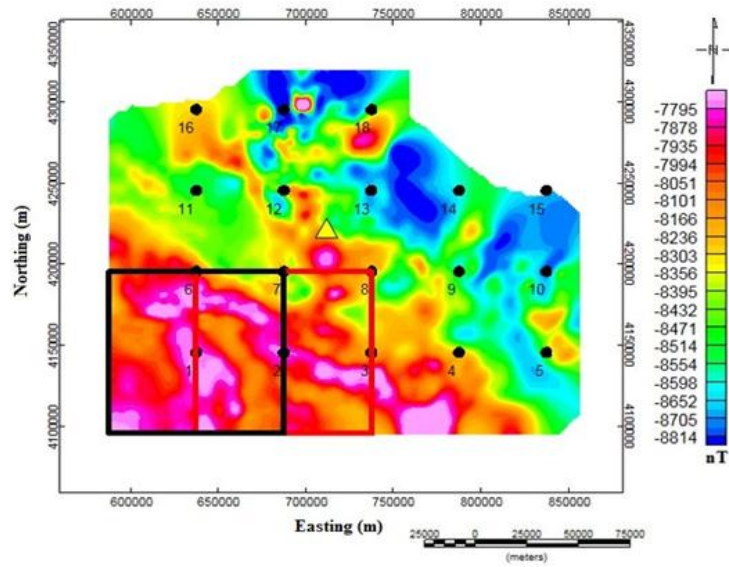
Figure 3. Selection of overlapping blocks on RTP map. Solid circles indicate centers of blocks (named as 1-18) and yellow solid triangle indicate Mt. Sabalan.
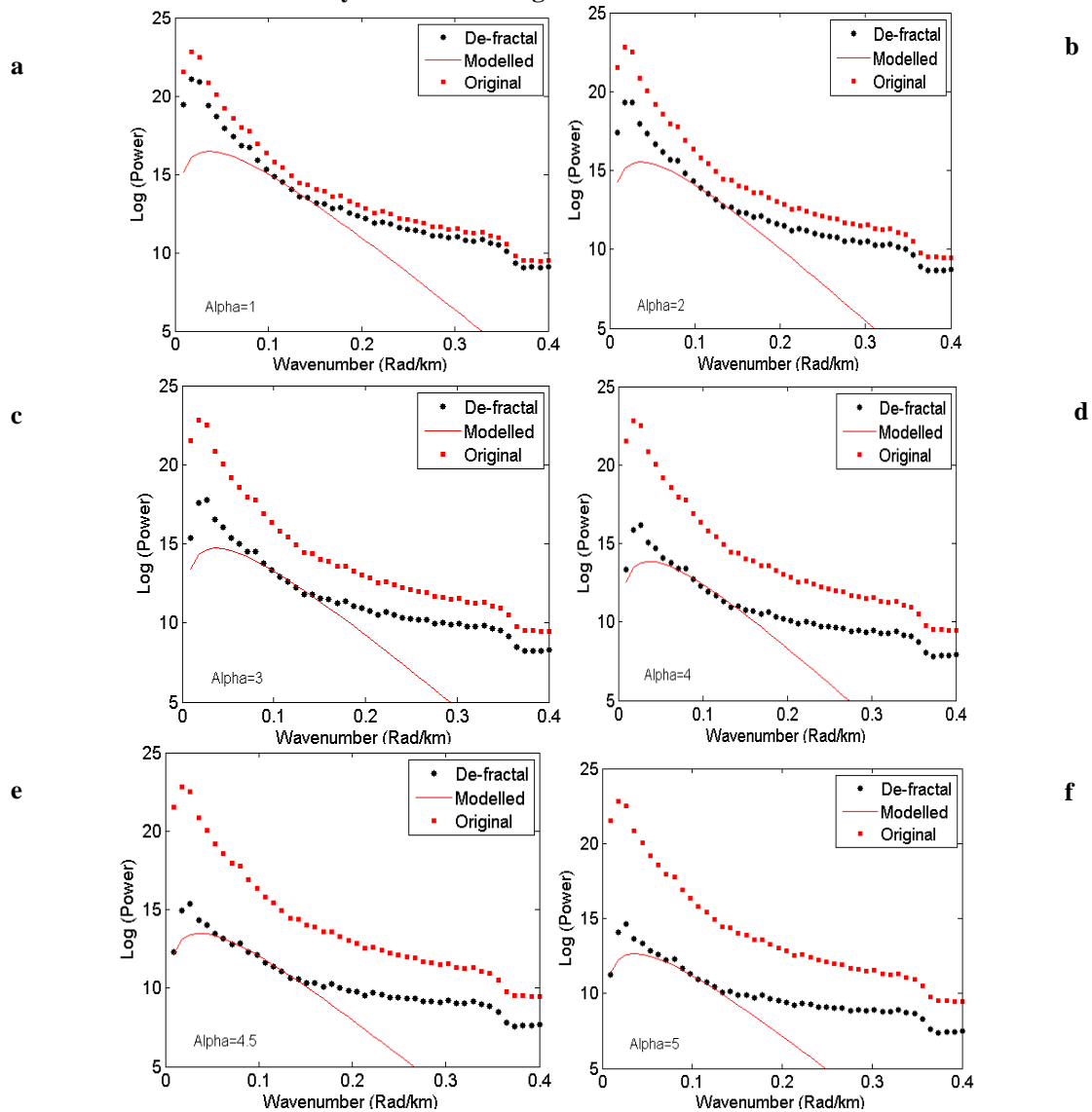
Figure 4. Comparison of de-fractal power spectra for block 4 using different α values (1, 2, 3, 4, 4.5, and 5) and modelled curves produced using best fit estimated parameters.

Table 2. Results of estimating depth to top and bottom of magnetic layer in Ardabil area.

Block number	Coordinates(UTM)		Fractal parameter (α)	Depth to top (km)	Depth to bottom (km)
	Easting (m)	Northing (m)			
1	637367	4145618	3.9	4.3	11.6
2	687367	4145618	4.2	5.0	12.8
3	737367	4145618	4.2	4.5	12.9
4	787367	4145618	4.5	3.2	14.2
5	837367	4145618	3.9	3.5	16.0
6	637367	4195618	4.4	2.9	13.4
7	687367	4195618	3.8	4.2	14.8
8	737367	4195618	4.1	4.5	15.1
9	787367	4195618	4.2	3.4	17.6
10	837367	4195618	4.0	2.9	18.0
11	637367	4245618	3.8	3.6	12.2
12	687367	4245618	4.1	4.7	10.6
13	737367	4245618	3.9	3.6	10.4
14	787367	4245618	3.7	2.3	18.9
15	837367	4245618	3.9	1.9	17.8
16	637367	4295618	4.1	3.1	19.3
17	687367	4295618	3.9	2.9	21.1
18	737367	4295618	4.0	4.1	20.9
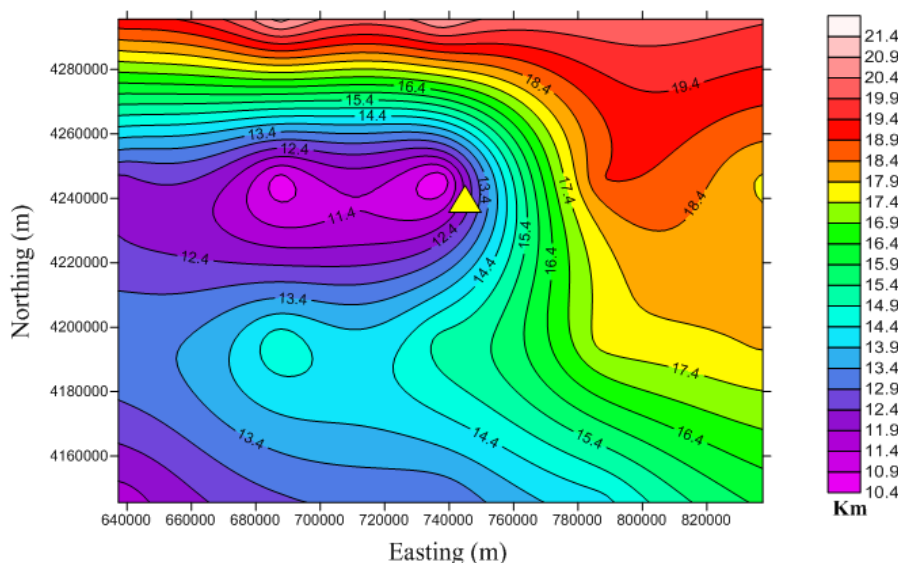
Figure 5. Bottom depth map of studied area (contour interval is 0.5 km) and location of Mt. Sabalan (yellow solid triangle).

References

[1]. Mandelbrot, B. B. (1983). The Fractal Geometry of Nature, W. H. Freeman, San Francisco.

[2]. Bansal, A.R., Gabriel, G, and Dimri, V.P. (2010). Power law distribution of susceptibility and density and its relation to seismic properties: An example from the German Continental Deep Drilling Program: Journal of Applied Geophysics. 72 (2): 123-128.

[3]. Fedi, M., Quarta, T. and De Santis, A. (1997). Improvements to the Spector and Grant method of source depth estimation using the power law decay of magnetic field power spectra, Geophysics. 62: 1143-1150.

[4]. Spector, A. and Grant, F.S., (1970). Statistical Models for Interpreting Aeromagnetic Data, Geophysics. 35: 293-302.

[5]. Pilkington, M. and Todoeschuck, J.P. (1993). Fractal magnetization of continental crust, Geophys. Res. Lett. 20: 627-630.

[6]. Pilkington, M., Todoeschuck, J.P. and Gregotski, M.E. (1994). Using fractal crustal magnetization models in magnetic interpretation, Geophysical Prospecting. 42: 677-692.

[7]. Maus, S. and Dimri, V.P. (1995). Potential field power spectrum inversion for scaling geology, J. Geophys. Res. 100: 12605-12616.

[8]. Maus, S., Gordon, D. and Fairhead, D. (1997). Curie temperature depth estimation using a self-similar magnetization model, Geophys. J. Int. 129: 163-168.

[9]. Ravat, D., Pignatelli, A., Nicolosi, I. and Chiappini, M. (2007). A study of spectral methods of estimating the depth to the bottom of magnetic sources from near-surface magnetic anomaly data, Geophys. J. Int. 169: 421-434.

[10]. Bouligand, C., Jonathan, M., Glen, G. and Blakely, J.R. (2009). Mapping Curie temperature depth in the western United States with a fractal model for crustal magnetization, J. Geophys. Res. 114: 1-25.

[11]. Bhattacharyya, B.K. and Leu, L.K. (1975). Spectral Analysis of Gravity and Magnetic Anomalies due to Two-dimensional Structures, Geophysics. 40: 993-1013.

[12]. Okubo, Y., Graf, R.J., Hansent, R.O., Ogawa, K. and Tsu, H. (1985). Curie point depths of the island of Kyushu and surrounding areas Japan, Geophysics.53: 481-494.

[13]. Shuey, R.T., Schellinger, D.K., Tripp, A.C. and Alley, L.B. (1977). Curie depth determination from aeromagnetic spectra, Geophys. J. Roy. Astr. Soc. 50: 75-101.

[14]. Blakely, R. (1988). Curie temperature isotherm analysis and tectonic implications of aeromagnetic data from Nevada, J. Geophys. Res. 93: 11817-11832.

[15]. Salem, A., Ushijima, K., Elsirafi, A. and Mizunaga, H. (2000). Spectral Analysis of Aeromagnetic Data for Geothermal Reconnaissance of Quseir area, Northern Red Sea, Egypt, Proceeding World Geothermal Congress, Kyushu, Japan. 1669-1674.

[16]. Bhattacharyya, B.K. and Leu, L.K. (1977). Spectral analysis of gravity and magnetic anomalies due to rectangular prismatic bodies, Geophysics. 41: 41-50.

[17]. Tanaka, A., Okubo,Y. and Matsubayashi, O. (1999). Curie point depth based on spectrum analysis of magnetic anomaly data in East and Southeast Asia, Tectonophysics. 306: 461-470.

[18]. Blakely, R.J. (1995). Potential theory in gravity and magnetic applications, Cambridge Univ. Press, Cambridge.

[19]. Bansal, A.R., Gabriel, G., Dimri, V.P. and Krawczyk, C.M. (2011). Estimation of depth to the bottom of magnetic sources by a modified centroid method for fractal distribution of sources: An application to aeromagnetic data in Germany, Geophysics. 76: 3: 11-22.

[20]. Salem, A., Green, C., Ravat, D., Singh, K.H., East, P., Fairhead, J.D., Mogren, S. and Biegert, E. (2014). Depth to Curie temperature across the central Red Sea from magnetic data using the de-fractal method. Tectonophysics. 75-86.

[21]. Ravat, D. (2004). Constructing full spectrum potential-field anomalies for enhanced geodynamical analysis through integration of surveys from different platforms (INVITED), EOS, Trans. Am. geophys. Un. 85 (47), Fall Meet. Suppl., Abstract G44A-03.

[22]. Finn, C.A. and Ravat, D. (2004). Magnetic Depth Estimates and Their Potential for Constraining Crustal Composition and Heat Flow in Antarctica, EOS, Trans. Am. geophys. Un, 85(47), Fall Meet. Suppl., Abstract T11A-1236.

[23]. Ross, H.E., Blakely, R.J. and Zoback, M.D. (2004). Testing the Utilization of Aeromagnetic Data for the Determination of Curie-Isotherm Depth, EOS, Trans. Am. geophys. Un., 85 (47), Fall Meet. Suppl., Abstract T31A-1287.

[24]. Connard, G., Couch, R., and Gemperle, M. (1983). Analysis of Aeromagnetic Measurements from Cascade Range in Central Oregon, Geophysics. 48: 376-390.

[25]. Ross, H.E., Blakely, R.J. and Zoback, M.D. (2006). Testing the use of aeromagnetic data for the determination of Curie depth in California: Geophysics. 71 (5): L51-L59.

[26]. Pilkington, M. and Todoeschuck, J.P. (1995). Scaling nature of crustal susceptibilities. Geophys. Res. Lett. 22: 779-782.

[27]. Maus, S. and Dimri, V.P. (1994). Scaling properties of potential fields due to scaling sources. Geophys. Res. Lett. 21: 891-894.

[28]. SKM (Sinclair Knight Merz). (2005). Resource review of the Northwest Sabalan geothermal project. Report submitted to SUNA. 61P.

[29]. KML. (1998). Sabalan geothermal project, stage 1-Surface exploration, final exploration report. Kingston Morrison Limited Co., report 2505-RPT-GE-003 for the Renewable Energy Organization of Iran, Tehran. 83 P.

[30]. Okubo, Y., Matsushima, J. and Correia, A. (2003). Magnetic spectral analysis in Portugal and its adjacent seas, Phys. Chem. Earth. 28: 511-519.

[31]. Hisarli, Z.M., Dolmaz, M.N., Okyar, M., Etiz, A. and Orbay, N. (2011). Investigation into regional thermal structure of the Thrace Region, NW Turkey, from aeromagnetic and borehole data, Stud. Geophys. Geod. 56: 269-291.

[32]. Ghaedrahmati, R., Moradzadeh, A., Fathianpour, N., Lee, S.K. and Porkhial, S. (2013). 3-D inversion of MT data from the Sabalan geothermal field, Ardabil, Iran, Journal of Applied Geophysics. 93: 12-24.

تعیین پارامتر فرکتالی و عمق منابع مغناطیسی منطقه زمین‌گرمایی اردبیل با استفاده از داده‌های مغناطیس هوایی

الله‌یار خوجملی*۱، فرامرز دولتی اردهجانی۲، علی مراد زاده۲، علی نجاتی کلاته۱، امین روشندل کاهو۱ و سهیل پرخیال۳

۱- دانشکده مهندسی معدن، نفت و ژئوفیزیک، دانشگاه صنعتی شاهرود، ایران

۲- دانشکده فنی و مهندسی، دانشکده معدن، دانشگاه تهران، ایران

۳- بخش انرژی زمین‌گرمایی سازمان انرژی‌های نو، وزارت نیرو، ایران

* نویسنده مسئول مکاتبات: akhojamli@shahroodut.ac.ir

چکیده:

میدان زمین‌گرمایی اردبیل در شمال غرب ایران و در اطراف کوه سبلان واقع شده است. این منطقه دارای گرادیان حرارتی و جریان حرارتی بسیار بالایی است. هدف از این مطالعه، تعیین پارامتر فرکتالی و عمق‌های بالایی و کف منابع مغناطیسی است. بدین منظور، از روش تحلیل طیفی اصلاح شده «طیف غیر فرکتال شده» استفاده شد. این روش ابتدا اثر فرکتالی مغناطیدگی طیف مشاهده شده را حذف کرده و سپس با استفاده از روش مدل‌سازی پیشرو پیک طیفی اقدام به تخمین عمق بالایی و کف منابع مغناطیسی می‌نماید. این روش بر روی داده‌های مغناطیس هوایی استان اردبیل بکار برده شد. نتایج به دست آمده نشان می‌دهند که عمق پایینی منابع مغناطیسی از ۱۰/۴ کیلومتر در شمال غرب سبلان تا حدود ۲۱/۱ کیلومتر در شمال منطقه مورد مطالعه تغییر می‌کند. علاوه بر این مقادیر پارامتر فرکتالی برای منطقه مورد مطالعه بین ۳/۷ تا ۴/۵ تعیین شدند.

کلمات کلیدی: پارامتر فرکتالی، داده‌های مغناطیس هوایی، میدان زمین‌گرمایی، منابع میدان مغناطیسی، طیف توان، سبلان.